

## Research Paper

**Cite this article:** Kadu MB, Rayavarapu N (2021). Compact stack EBG structure for enhanced isolation between stack patch antenna array elements for MIMO application. *International Journal of Microwave and Wireless Technologies* **13**, 817–825. <https://doi.org/10.1017/S1759078720001543>

Received: 20 April 2020

Revised: 22 October 2020

Accepted: 22 October 2020

First published online: 18 November 2020


### Key words:

Electromagnetic bandgap structure; isolation; MIMO; stack antenna

### Author for correspondence:

M. B. Kadu, E-mail: [maresh.kadu@gmail.com](mailto:maresh.kadu@gmail.com)

# Compact stack EBG structure for enhanced isolation between stack patch antenna array elements for MIMO application

Mahesh B. Kadu<sup>1</sup>  and Neela Rayavarapu<sup>2</sup>

<sup>1</sup>Research Scholar, Symbiosis International (Deemed University), Lavale, Pune, India and <sup>2</sup>Symbiosis Institute of Technology, Symbiosis International University, Symbiosis International (Deemed University), Lavale, Pune, India

## Abstract

In this research article, a compact wideband stack patch antenna array integrated with compact stack electromagnetic band gap (EBG) structure for multiple input multiple output (MIMO) application is proposed. The wide resonance bandwidth is achieved at 2.45 GHz band by stack arrangement of compact meander line slot driven and parasitic patch elements. The isolation bandwidth is matched with resonance bandwidth with the design of a compact stack L slot EBG structure. The polarization diversity and three-layer EBG structure ensure an enhancement in isolation level. To validate the performance of the proposed stack antenna array, a prototype was fabricated and tested for different MIMO parameters. The measured result confirms the effectiveness of the proposed antenna array in a diverse MIMO environment.

## Introduction

The microstrip patch antenna arrays have been adopted widely for a range of multiple input multiple output (MIMO) wireless devices. However, due to the compact nature of wireless devices; the antenna elements in an array have to be closely spaced. This results in the increased mutual coupling between antenna elements, leading to degradation in antenna performance. The size of the antenna plays a crucial role in the design of MIMO antenna arrays for compact wireless devices, as the compact size of the antenna will allow greater spacing between antenna elements compared to conventional antennas. Different types of compact antenna designs, such as design using a dielectric substrate of high permittivity [1], design with a slot on the patch [2] and design with a destructive ground structure (DGS) or a combination of these have been reported in the literature [3].

However, miniaturization of microstrip antenna (MSA) causes the resonance bandwidth to shrink to some extent as the quality factor increases during the process. This raises new challenges in compact antenna design, and a tradeoff must exist between the size and bandwidth. A monopole antenna designed with a DGS has been very popular in recent years due to its larger bandwidth and compact size. However, it does not exhibit a stable radiation pattern over its operating frequency. In this paper, a novel compact stack configuration of compact patch elements is proposed. This method utilizes the space in vertical direction available in a device, ensures that the size in the horizontal direction is the same as of the compact patch antenna. Thus, this stack antenna is appropriate to be used as array elements. Isolation between array elements can be enhanced by cutting off the coupling path between the ports of the elements. A majority of researchers have developed different substrate surface wave mitigation techniques. In one of isolation enhancement techniques, DGS is introduced by purposely changing the ground plane of the MGS array [4]. However, change of the ground plane may perturb the antenna's radiation pattern and also effect in reduced gain. Isolation between the ports can also be enhanced by mitigating the space waves using metamaterials [5], use of stub loading technique [6], introducing the neutralizing line in array design [7] and shorting pins [8]. Electromagnetic band gap (EBG) structures in an antenna array provide the isolation between antenna elements for a given band gap [9]. To mitigate the mutual coupling through space waves, diversity reception techniques have been applied. The space diversity technique offers the simplest solution. However, the compact nature of wireless devices puts a limitation on the maximum spacing between the antenna elements. Another such technique is polarization diversity where two elements radiate at orthogonal polarizations with respect to each other [10].

The main challenge for this work is to discover strategies to simultaneously address the aforementioned issues of compact size, wide bandwidth, and high isolation. The contribution of the authors includes the design of a novel compact stack antenna with compact size and

wide bandwidth, design of compact stack EBG structure for enhanced isolation and high bandwidth.

### Stack antenna design

The driven and parasitic patch elements of stack antenna are designed with FR4 substrate having dielectric constant ( $\epsilon_{r1}$  and  $\epsilon_{r3} = 4.4$ ), loss tangent 0.02 and height  $h = h1 = h3 = 1.6$  mm. The substrate on which the parasitic patch is etched is placed with an air gap  $h2 = 5$  mm from a driven patch. The air gap acts as a dielectric substrate with dielectric constant  $\epsilon_{r2} = 1$ . The driven patch is driven with a coaxial line feed and the electromagnetic coupling with a driven patch excites the top parasitic patch as seen in Fig. 1(a). A shorting pin introduced in the antenna design enhances the coupling between the patches due to the physical connection between the two patch elements and also provides physical rigidity to the antenna, compared to conventional stack design. Both, the driven and parasitic patches are designed with half of the dimension of the conventional patch by introducing a meander line structure as depicted in Fig. 1(b). The driven and parasitic patches are designed with a substrate length ( $L$ ) = 24 mm and width ( $W$ ) = 30 mm. While the driven patch is optimized with dimensions of length of patch ( $l_p$ ) = 16.5 mm, width of patch ( $w$ ) = 22 mm, feed position fixed to ( $x$ ) = 6.25 mm and short at  $y = 1.75$  mm. Whereas parasitic patch dimensions are optimized to  $l = 14$  mm and width  $w = 22$  mm. The gap  $S$  between meander line elements is obtained to be 2.2 mm and width of meander line arm to  $a = 1$  mm for both driven and parasitic patch elements.

Thus, tuning of lower resonant frequency with the change in inductance for stack patch antenna is realized by variation of meander line arm length  $l$  for the driven patch as demonstrated in Fig. 2(a). Whereas, the tuning of the upper resonant frequency of the stack antenna is dictated by the length  $l$  of the meander line arm of the parasitic patch as shown in Fig. 2(b). The combined tuning of resonance of the driven and parasitic patches by variation of length of meander line arm achieves the desired resonance bandwidth for the stacked antenna.

### Design of high isolation stack antenna array with stack EBG

To mitigate space wave coupling polarization diversity proves to be an effective solution. The two antenna elements of stacked antenna sharing a common substrate are aligned to generate orthogonal polarization to each other. The current distribution in Fig. 3 shows that the electric fields of antenna elements are oriented orthogonal to each other. The antenna 1 orients the field in a vertical direction, whereas for antenna 2 the electric field vectors are in the horizontal direction. Figure 4(b) demonstrates a reduction of 8 dB mutual coupling with the introduction of polarization diversity between driven as well as parasitic elements of the stack antenna.

### Design of compact L slot EBG

The dimensions of the EBG element are a function of its wavelength, which in turn is inversely proportional to the equivalent inductance and capacitance of EBG. Therefore, to provide a realistic solution for a compact EBG design the process for increasing series inductance is realized using the L slot EBG structure [11] as shown in Fig. 5(a). The single unit of L slot EBG is designed with a substrate dielectric of FR4 with a relative permittivity of 4.4 and

a loss tangent of 0.02. The height of the substrate is 1.6 mm. The corresponding optimized parameters are  $p1 = 7$  mm,  $p2 = 4.8$  mm, and  $p = 0.8$  mm, respectively. Whereas the L slot is constructed with the width  $u = 0.7$  mm.

An L slot EBG layer 1 of  $2 \times 4$  EBG elements arranged as seen in Fig. 5(b) is placed at the center of two array antenna elements with dimensions of  $W_e = 12.3$  mm and  $L_e = 29.5$  mm, the distance between two adjacent EBG element optimized to  $k = 0.5$  mm. The stop band of EBG structure can be determined with a very powerful analysis tool termed as a dispersion diagram. The dispersion diagram is obtained from the inbuilt eigenmode solver feature of Ansoft high-frequency structure simulator (HFSS) software. The simulation utilizes the Brillouin diagram to determine the stop-band of a periodic structure. The advantage is that we can determine the stop band of the entire periodic EBG layer by analyzing a single unit cell. The airbox is used to cover a single unit cell of EBG as shown in Fig. 6(a). It has the same length and width as the EBG unit cell. The height of the airbox is six times the thickness of the substrate material. Then perfect matched layer boundary conditions are defined for the airbox [12]. Finally, the dispersion diagram was computed along the edges of the irreducible Brillouin zone, following the triangle with the points  $\Gamma$ ,  $X$ , and  $M$  [12]. The dispersion diagram of the L slot EBG is depicted in Fig. 6(b) verifies the presence of stop band in proposed L slot EBG.

### Design of stack L slot EBG

The isolation bandwidth and amount of isolation offered by the L slot EBG layer 1, discussed in the section above are not enough to match the requirement of a stack antenna array. The limited space available for placement of EBG elements between the patch antennas restricts the increase of both columns and rows of EBG elements in layer 1. This, in turn, puts a limitation on amount and bandwidth of isolation. To overcome this issue a novel stack EBG configuration is proposed in this work. Figure 4(a) demonstrates the proposed three layers of L slot EBG stack structure. EBG layer 1 consists of  $2 \times 4$  elements etched on the same substrate as that of the driven patch antenna, with each of the dimensions as depicted in Fig. 5(b). EBG layer 2 of dimensions same as of layer 1 is etched on the upper substrate between parasitic patch elements. The third EBG layer designed in similarity with layers 1 and 2 is etched on a separate FR4 substrate of dimensions of  $W_e = 12.3$  mm and  $L_e = 29.5$  mm, placed and aligned with EBG layer 1, with an air gap of 0.4 mm between layer 1 and substrate of layer 3. A shorting pin connects EBG layers 1 and 3 with the ground element. The coupling between the different layers of EBG results in increasing the overall height  $H$  of EBG, leading to an increase in the inductance of EBG ( $L_{ebg}$ ), which is directly proportional to isolation bandwidth ( $B.W_I$ ) as demonstrated in equations (1) and (2).

$$B.W_I = \frac{1}{120\pi} \sqrt{\frac{L_{ebg}}{C_{ebg}}} \quad (1)$$

$$L_{ebg} = \mu_0 H \quad (2)$$

The coupling between the three EBG layers provides the desired height. Thus, the novel stack structure widens the bandwidth without increasing the space in the horizontal direction compared to

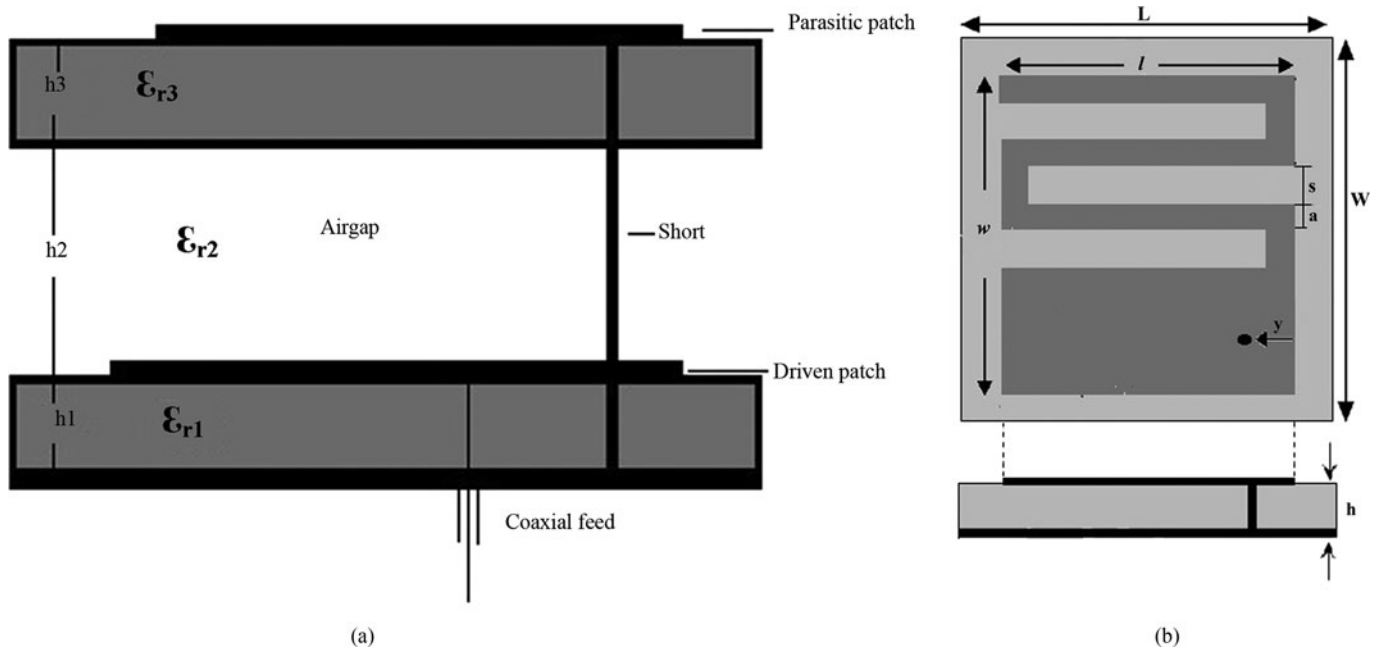


Fig. 1. (a) Side view of stack antenna. (b) Cross sectional view of compact patch.

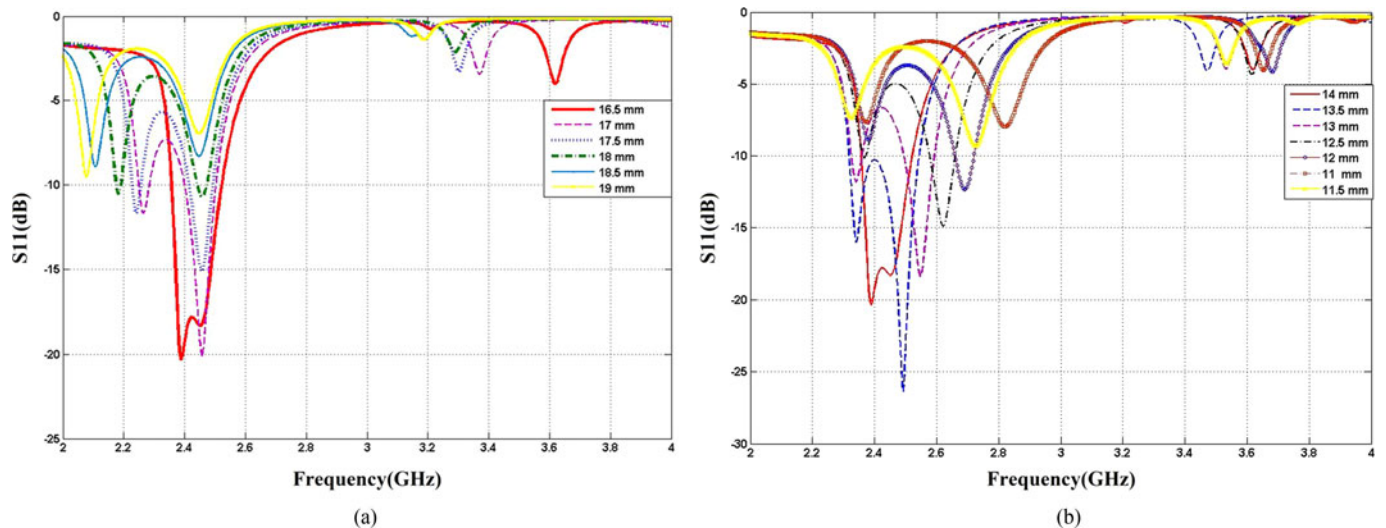


Fig. 2. (a) Lower frequency tuned with meander line arm length of driven patch element. (b) Upper resonant frequency tuned with meander line arm length of parasitic patch element.

the conventional arrangement of EBG elements. The increase in isolation bandwidth with each EBG layer is demonstrated in Fig. 4(b). The result shows an improvement of 10 dB in mutual coupling with the inclusion of EBG structure in the antenna array.

### Results and discussion

#### Return loss

The photograph of the prototype is shown in Fig. 7(a). For verification of performance, the prototype stack antenna was tested by a 2-port Agilent E5080A network analyzer, while the simulated

reflection coefficient ( $S_{11}$ ) is obtained from ANSYS HFSS simulation software using a solution data report feature. The simulated and measured reflection coefficients of the proposed stack antenna are shown in Fig. 7(b). It shows that the simulated reflection coefficient is lower than 10 dB in the desired band of operation. The measured resonance band is from 2.37 to 2.54 GHz which is very close to the simulated frequency band. To confirm that the EBG structure in an array does not hamper the individual performance of the stack antenna, the reflection coefficient is measured again for the antenna elements in the array as depicted in Fig. 8(b). Return loss parameters of both antenna elements overlap each other due to the symmetric nature of array design.

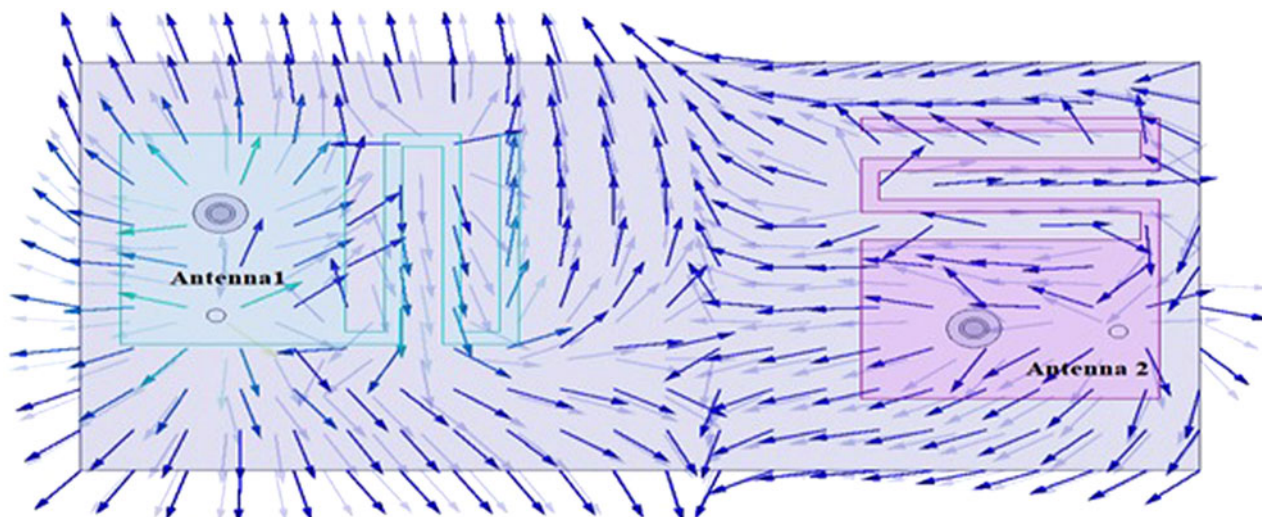


Fig. 3. Electric field orientation with polarization diversity introduced in array structure.

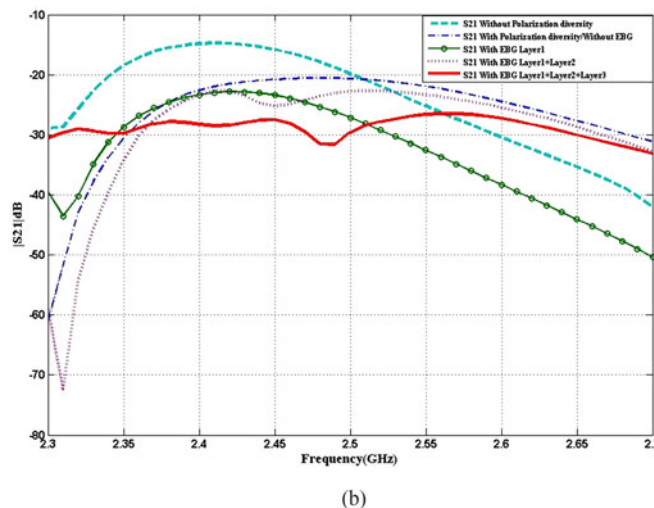
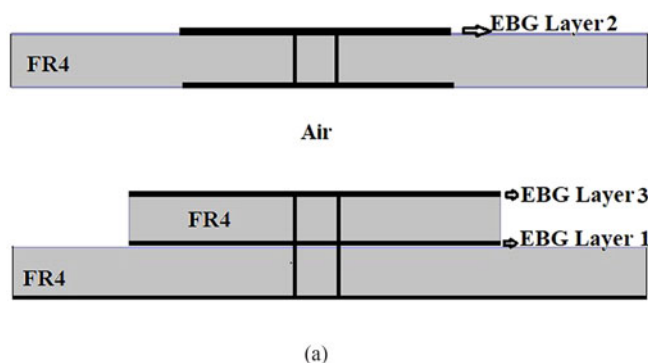


Fig. 4. (a) Side view of stack EBG structure. (b) Mutual coupling  $S_{21}$  (dB) versus frequency.

Although, a little difference in simulated and measured results is observed due to the connector soldering effects.

**Isolation**

The combined effect of polarization diversity and stack L slot EBG structure results in mutual coupling reduction of 18 dB and thus results in enhancement of isolation between ports 1 and 2 of the stack antenna array. For validating these results, a  $2 \times 1$  stack antenna array with stack L slot EBG structure was fabricated as depicted in Fig. 8(a). The scattering parameters of array structure were measured with two port vector network analyzer in an open area test site. The measured and simulated return loss and coupling parameters are plotted in Fig. 8(b). It can be seen that mutual coupling values are well below 29 dB in the desired band, for both the simulated and measured results. A slight variation of the measured result is seen as compared to simulated result. This variation can be accepted within a tolerance value.

**MIMO parameters**

The proposed array antenna was tested for different MIMO performance parameters such as envelope correlation coefficient (ECC), total active reflection coefficient (TARC), diversity gain (D. G), and mean effective gain (MEG). This section includes the mathematical equations that can be defined as an output variable in HFSS to obtained the MIMO performance parameters.

**Envelope correlation coefficient and total active reflection coefficient**

Isolation between ports of an antenna array is represented by the ECC value. The acceptable limit of ECC for good quality diversity performance is below 0.5. The ECC value can be calculated from S-parameter values as given in equation (3) below.

$$ECC = \frac{|S_{11}^* S_{12} + S_{21}^* S_{22}|^2}{((1|S_{11}|^2|S_{21}|^2)(1|S_{22}|^2|S_{12}|^2))} \tag{3}$$

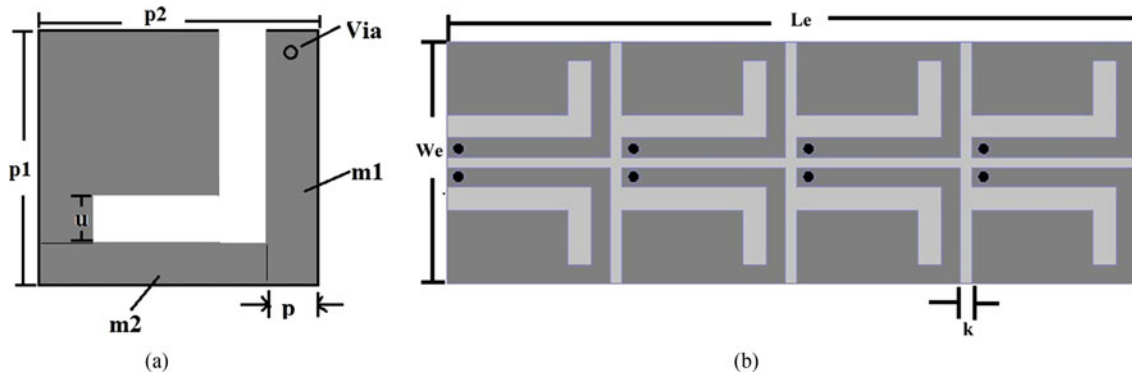


Fig. 5. (a) Top view of L slot EBG. (b) L slot EBG layer 1.

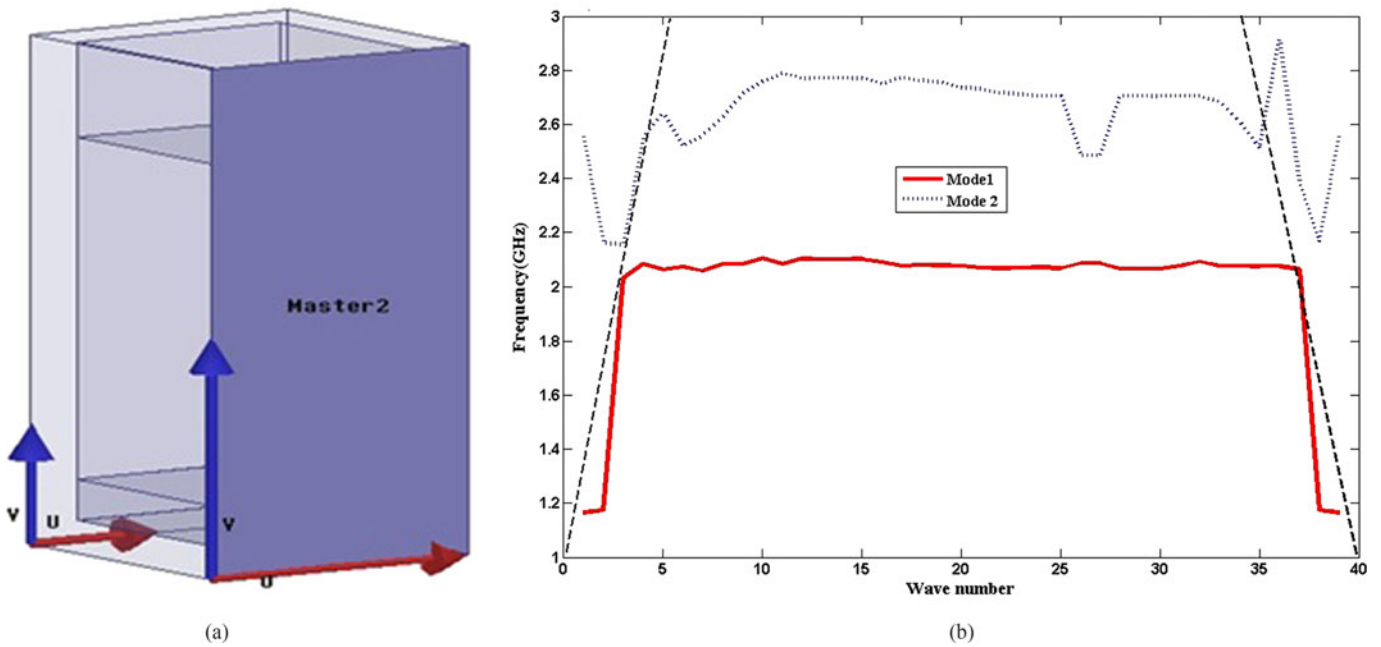


Fig. 6. (a) Simulation setup for dispersion diagram measurement. (b) Dispersion diagram for L slot EBG.

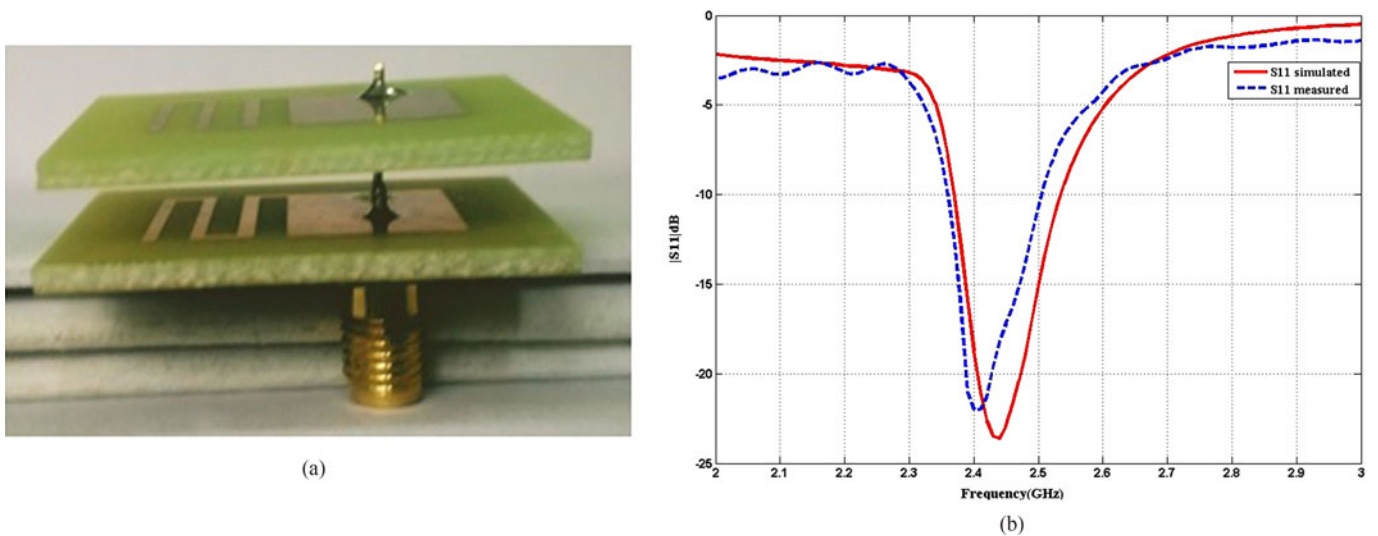
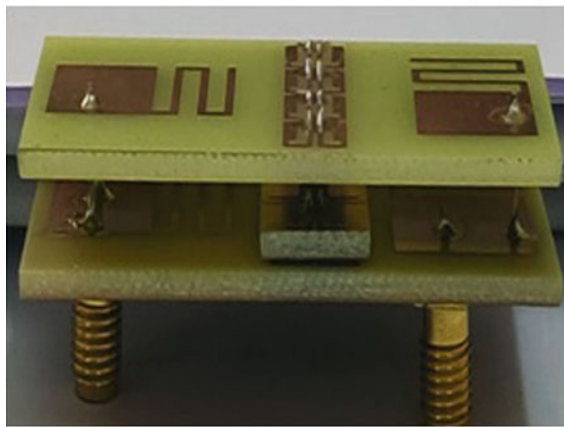
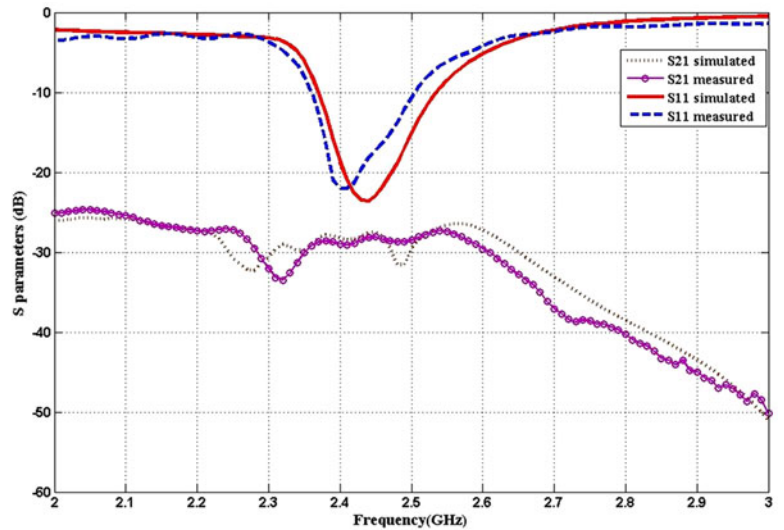


Fig. 7. (a) Side view of stack antenna. (b) Return loss versus frequency.

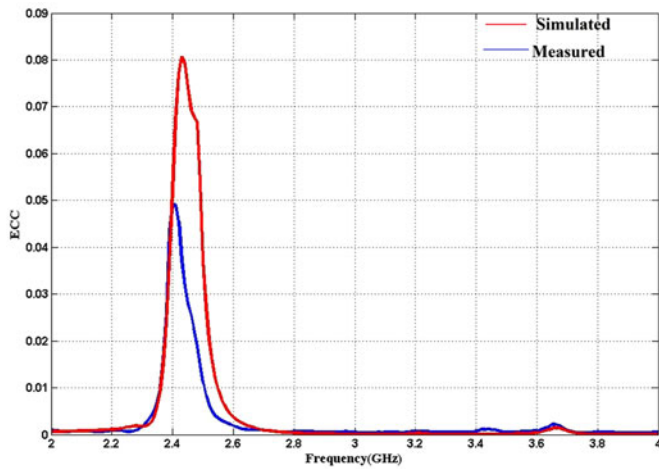


(a)

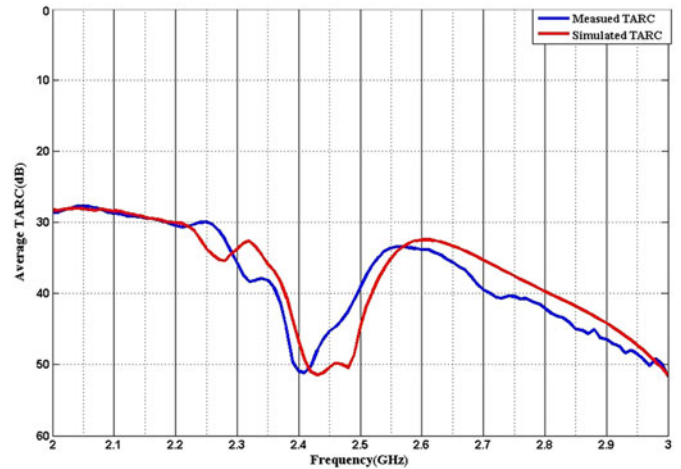


(b)

Fig. 8. (a) Side view of stack antenna array. (b) Scattering parameters for stack antenna array embedded with L slot EBG structure.



(a)



(b)

Fig. 9. (a) Plot of ECC with frequency. (b) Plot of TARC with frequency.

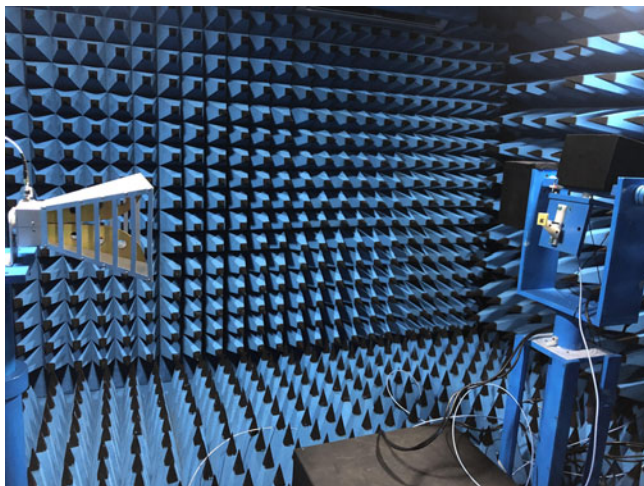


Fig. 10. Anechoic chamber radiation pattern measurement setup.

where  $S_{11}$  and  $S_{22}$  are the return loss values for ports 1 and 2, respectively, while  $S_{21}$  and  $S_{12}$  denote the inter port coupling of the array antenna. Both the simulated and measured S parameters are used to compute simulated and measured values of ECC. The value of ECC in the frequency range is well below 0.08 as seen in Fig. 9(a). TARC is derived by combining the effects of both isolation and diversity for a MIMO antenna array. TARC value can be calculated by the S parameters obtained from both simulation and measurement as from equation (4).

$$\Gamma_a^t = \frac{\sqrt{|S_{11} + S_{12}e^{j\theta}|^2 + |S_{21} + S_{22}e^{j\theta}|^2}}{\sqrt{2}} \quad (4)$$

The average value of TARC derived from simulated and measured S parameters is depicted in Fig. 9(b). The TARC value averaged over different values of  $\theta$  is well below the acceptable limit of 30 dB.

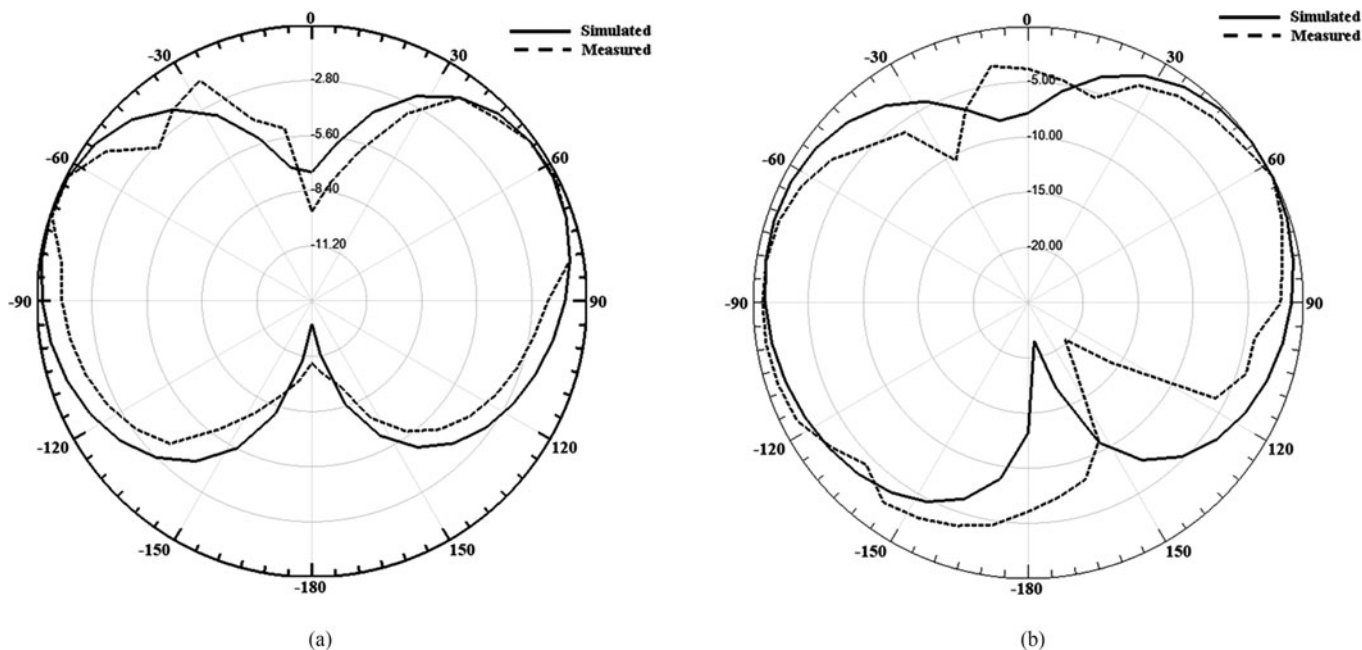


Fig. 11. Radiation pattern for stack antenna embedded without stack L slot EBG at 2.45 GHz; (a)  $E$  plane at  $\phi = 0^\circ$ , (b)  $H$  plane at  $\phi = 90^\circ$ .

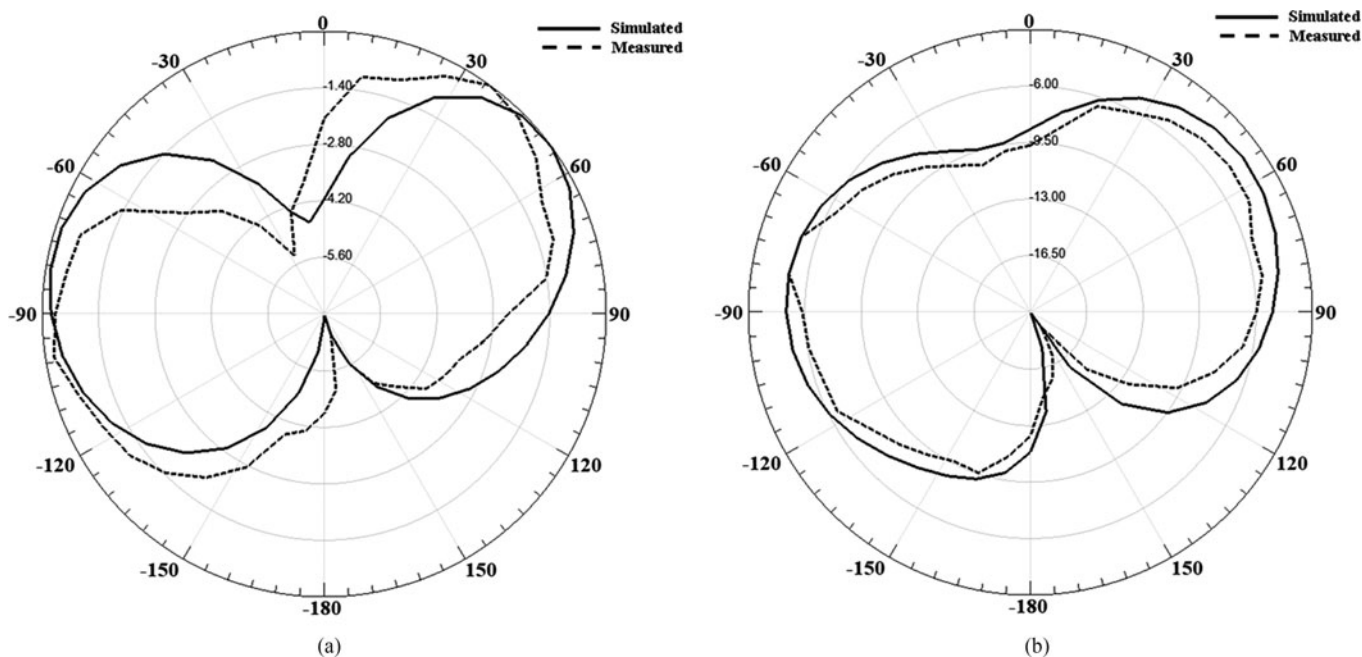


Fig. 12. Radiation pattern for stack antenna embedded with stack L slot EBG at 2.45 GHz; (a)  $E$  plane at  $\phi = 0^\circ$ , (b)  $H$  plane at  $\phi = 90^\circ$ .

**D. G and MEG**

D. G <deleted redundancy text> is the most popular technique defining the diversity performance of MIMO antenna array and its value can be computed by equation (5) given below.

$$D.G = 10 \times \sqrt{(1|0.99ECC|^2)} \tag{5}$$

Its maximum value obtained for a practical MIMO antenna array is 10 dB. The proposed antenna array presents the DG

value obtained from simulation below 9.98 dB. The measured value is well below 9.96 dB for a given frequency band. MEG is one of the vital parameters for measuring diversity performance in a MIMO system. It is usually defined relative to the isotropic antenna. Mathematically, it is defined as

$$MEG_i = 0.5 \times \left( 1 - \sum_j^N |S_{ij}|^2 \right) \tag{6}$$

Table 1. Comparison of the proposed design with previous designs

References	[15]	[16]	[17]	[18]	[19]	[20]	[21]	[22]	[23]	[24]	Proposed design
Size of antenna array	$1.12\lambda_0 \times 1.43\lambda_0$	$0.58\lambda_0 \times 1.0\lambda_0$	$0.70\lambda_0 \times 0.95\lambda_0$	$0.81\lambda_0 \times 0.5\lambda_0$	$0.48\lambda_0 \times 0.3\lambda_0$	$0.42\lambda_0 \times 0.5\lambda_0$	$0.63\lambda_0 \times 0.83\lambda_0$	$0.34\lambda_0 \times 0.31\lambda_0$	$0.46\lambda_0 \times 0.46\lambda_0$	$0.56\lambda_0 \times 0.50\lambda_0$	$0.24\lambda_0 \times 0.50\lambda_0$
Decoupling mechanism	DGS	Metal plates	EBG	DGS	CSRR	Meta-material	EBG	Meta-material	Meta-material	Meta-material	EBG
Isolation bandwidth %	06	07	02	04	03	03	03	05	03	02	13
Mutual coupling [dB]	>30	>23	>20	>20	>30	>15	>20	>24	>18	>24	>29
Antenna bandwidth %	08	12	03	04	04	04	04	05	02	02	11
Substrate type	FR4	Taconic RF-35	FR4	Roger 4350	FR4	FR4	FR4	Rogers RT/Duroid 5880	FR4	FR4	FR4
Gain of antenna [dB]	5	5	1.6	1	1.95	2.0	6	7.5	5	2	2.15
Flexibility	Less	Less	More	More	Less	Less	Less	Less	More	More	More
ECC	N/G	0.09	0.03	0.03	N/G	N/G	N/G	0.05	0.03	0.03	0.06

where  $i$  represents the port at which *MEG* is measured and  $N$  represents the number of ports. The desired value of the difference between *MEG*<sub>1</sub>, for the port of antenna element 1 and *MEG*<sub>2</sub>, derived for the port of antenna element 2 should be within 3 dB for the similar input power at both the ports. The ratio of *MEG*<sub>1</sub>/*MEG*<sub>2</sub> is found to be 0.96 by measurement and 0.98 by simulation data of  $S$  parameters.

*Radiation pattern*

The stack antenna is designed to exhibit a bidirectional radiation pattern as the intended application is a MIMO system that supports a multipath environment and the antenna must be capable of receiving signals in all possible directions. The 2D far-field radiation pattern at 2.45 GHz for single stack antenna without L slot EBG layer is plotted with both simulated and measured values obtained from measurement setup depicted in Fig.10 is shown in Fig. 11. It is plotted with  $\theta$  variation from 0° to 360° on  $\phi = 0^\circ$  and  $\phi = 90^\circ$  plane and uses the far-field simulation feature of HFSS and anechoic chamber facility for measured results. The stack design yields a bidirectional pattern due to the presence of multiple radiating patches arranged in a stack configuration [13, 14]. Figure 12 depicts the radiation plot of the stack antenna element in a 2 × 1 antenna array in the presence of stack L slot EBG structure. It is found that the stack antenna radiation pattern has a modest variation with the inclusion of the EBG layer in between the two antenna elements. Due to the symmetry property of the stack antenna, the other port exhibits similar radiation patterns.

*Comparative analysis*

A comparison of the proposed design and previous designs reported in the literature is tabulated in Table 1. It is to be noted that the lowermost frequency band is considered for calculation for free-space wavelength  $\lambda_0$ , in the case of the multiband antenna configuration. As seen from the comparison in Table 1, the proposed design offers a high isolation, wide isolation bandwidth and compact array design in the horizontal plane along with flexibility in design, manufactured with the economical substrate and better MIMO performance.

**Conclusion**

This research work has resulted in the design of a compact high isolation stack antenna array for a MIMO application by incorporating a stack EBG structure. First, a compact stack patch antenna was designed using the FR4 substrate with a dielectric constant of 4.4 resonating at 2.45 GHz frequency band over a wider bandwidth. Later, a stack antenna array embedded with stack L slot EBG structure was designed. The isolation level between two elements of the stack array was enhanced to 18 dB over a bandwidth of 13% by introducing polarization diversity and a wideband stack L slot EBG structure between individual antenna elements. Hence the proposed design is a good candidate for compact wireless devices working in a MIMO environment.

**References**

1. Fukusako T and Nakano T (2015) A compact patch antenna using artificial ground structure with high permittivity substrate. *IEEE-APS Topical Conference on Antennas and Propagation in Wireless Communications*, Turin.



2. **Jolani F and Dadgarpour AM** (2008) Compact M-slot folded patch antenna for WLAN. *Progress in Electromagnetics Research Letters* **3**, 35–42.
3. **Dasari N and Karunakar G** (2018) Compact printed elliptical microstrip patch with defected ground structure (DGS) for wireless applications. *International Journal on Communications Antenna and Propagation* **8**, 271–276.
4. **Kamal S and Chaudhari A** (2017) Printed meander line MIMO antenna integrated with air gap, DGS and RIS: a low mutual coupling design for LTE applications. *Progress in Electromagnetics Research C* **71**, 149–159.
5. **Qiu Y, Peng L, Jiang X, Sun Z and Tang S** (2017) Ultra-small single-negative metamaterial insulator for mutual coupling reduction of high-profile monopole antenna array. *Progress in Electromagnetics Research C* **72**, 197–205.
6. **Liao W-J, Chang S-H, Yeh J-T and Hsiao B-R** (2014) Compact dual-band WLAN diversity antennas on USB dongle platform. *IEEE Transactions on Antennas and Propagation* **62**, 109–118.
7. **Si-yan L, Xiao-lin L and Zu-fan Z** (2012) High isolation dual-element modified PIFA array for MIMO application. *The Journal of China Universities of Posts and Telecommunications* **19**, 1–6.
8. **Singh HS, Meruva BR, Pandey GK, Bharti PK and Meshram MK** (2013) Low mutual coupling between MIMO antennas by using two folded shorting strips. *Progress in Electromagnetics Research B* **53**, 205–221.
9. **Lee J-Y, Kim S-H and Jang J-H** (2015) Reduction of mutual coupling in planar multiple antenna by using 1-D EBG and SRR structures. *IEEE Transactions on Antennas and Propagation* **63**, 4191–4198.
10. **Femina BS and Mishra SK** (2016) Compact WLAN band-notched printed ultrawideband MIMO antenna with polarization diversity. *Progress in Electromagnetics Research C* **61**, 149–159.
11. **He H-S, Lai X-Q, Xu W-D, Jiang J-G, Zang M-X, Ye Q and Wang Q** (2011) Efficient EMI reduction in multilayer PCB using novel wideband electromagnetic bandgap structures. *International Journal of RF and Microwave Computer-Aided Engineering* **21**, 1–7.
12. **Anthony, RF & Microwave Engineering Tutorials/Tools**, Accessed on: 07. 03, 2020. [Online]. Available at [http://www.emtalk.com/tut\\_2.htm](http://www.emtalk.com/tut_2.htm).
13. **Keshari JP, Kanaujia BK, Khandelwal MK, Bakariya PS and Mehra RM** (2017) Omnidirectional multi-band stacked microstrip patch antenna with wide impedance bandwidth and suppressed cross-polarization. *International Journal of Microwave and Wireless Technologies* **9**, 629–638.
14. **Kumar A, Gupta N and Gautam PC** (2018) Design analysis of broadband stacked microstrip patch antenna for WLAN applications. *Wireless Pers Communication* **103**, 1499–1515.
15. **Chen ZN and Terence SP** (2011) Analysis and optimization of compact suspended plate MIMO antennas. *IEEE Transactions on Antennas and Propagation* **59**, 1–7.
16. **Tran HH, Hussain N and Le TT** (2019) Low-profile wideband circularly polarized MIMO antenna with polarization diversity for WLAN applications. *International Journal of Electronics and Communications* **11**, 172–180.
17. **Tu DTT, Van Hoc N, Son PD and Van Yem V** (2017) Design and implementation of dual-band MIMO antenna with low mutual coupling using electromagnetic band gap structures for portable equipments. *International Journal of Engineering and Technology Innovation* **7**, 48–60.
18. **Sharawi MS, Ikram M and Shamim A** (2017) A two concentric slot loop based connected array MIMO antenna system for 4G/5 G terminals. *IEEE Transactions on Antennas and Propagation* **65**, 6679–6686.
19. **Aminu-Baba M, Rahim MKA, Zubir F, Iliyasu AY, Fairus M, Yusoff M, Jahun KI and Ayop O** (2019) Compact patch MIMO antenna antennas with low mutual coupling for WLAN applications. *Journal of Electrical Engineering* **18**, 43–46.
20. **Luo S, Li Y, Xia Y, Yang G, Sun L and Zhao L** (2019) Mutual coupling reduction of a dual-band antenna array using dual-frequency metamaterial structure. *ACES Journal* **34**, 1–8.
21. **Naser-Moghadasi M, Ahmadian R, Mansouri Z, Zarrabi FB and Rahimi M** (2014) Compact EBG structures for reduction of mutual coupling in patch antenna MIMO arrays. *Progress in Electromagnetics Research C* **53**, 145–154.
22. **Mark R, Rajak N, Mandal K and Das S** (2019) Metamaterial based superstrate towards the isolation and gain enhancement of MIMO antenna for WLAN application. *International Journal of Electronics and Communications* **10**, 144–152.
23. **Yu K, Li Y and Liu X** (2018) Mutual coupling reduction of a MIMO antenna array using 3-D novel meta-material structures. *Applied Computational Electromagnetics Society Journal* **33**, 758–763.
24. **Ibrahim AA, Abdalla MA and Shubair RM** (2017) High-isolation metamaterial MIMO antenna. *IEEE International Symposium on Antennas and Propagation & USNC/URSI National Radio Science Meeting*, San Diego.



**Mahesh B. Kadu** is currently working as an assistant professor in Electronics and Telecommunication Department of Amrutvahini COE, Sangamner, MS, India. He is a Ph.D. research scholar at Symbiosis International (Deemed University), Lavale, Pune, India since 2015.



**Dr. Neela Rayavarapu** is currently head of the Electronics and Telecommunication department and a professor in Symbiosis Institute of Technology, Symbiosis International (Deemed University), Lavale, Pune, India. She is a registered Ph.D. guide with Electronics and Telecommunication Department, Symbiosis Institute of Technology, Symbiosis International (Deemed University), Lavale, Pune, India.